



## PERFORMANCE, EMISSION AND COMBUSTION CHARACTERISTICS OF BIOETHANOL-BIODIESEL-DIESEL FUEL BLENDS USED IN A COMMON RAIL DIESEL ENGINE

Hasan AYDOGAN

Selcuk University, Technology Faculty, Department of Mechanical Engineering, Konya, Turkey,  
haydogan@selcuk.edu.tr

(Geliş Tarihi: 13.01.2014, Kabul Tarihi: 17.09.2014)

**Abstract:** The changes in the performance, emission and combustion characteristics of bioethanol-safflower biodiesel and diesel fuel blends used in a common rail diesel engine were investigated in this experimental study. E20B20D60 (20% bioethanol, 20% biodiesel, 60% diesel fuel by volume), E30B20D50, E50B20D30 and diesel fuel (D) were used as fuel. The tests were performed at full-throttle valve opening and variable engine speeds. The results of the tests showed decreases in engine power, engine torque, carbon monoxide (CO), hydrocarbon (HC) and smoke density values with the use of bioethanol- biodiesel-diesel fuel blends, whereas, increases were observed in nitrogen oxide (NO<sub>x</sub>) and brake specific fuel consumption (BSFC) values. When combustion characteristics were examined, it was seen that the values were close to one another.

**Keywords:** Bioethanol, safflower biodiesel, common rail diesel engine, combustion characteristics

## BİYOETANOL-BİYODİZEL-DİZEL YAKITI KARIŞIMLARININ COMMON RAIL BİR DİZEL MOTORDA KULLANIMININ PERFORMANS, EMİSYON VE YANMA KARAKTERİSTİKLERİ

**Özet:** Sunulan deneysel çalışmada; common-rail püskürtme sistemine sahip bir dizel motorunda, biyoetanol-aspir biyodizeli-dizel yakıtı karışımlarının kullanılmasının motor performans parametreleri, egzoz emisyonları ve yanma karakteristikleri üzerindeki etkileri deneysel olarak incelenmiştir. Yakıt olarak E20B20D60 (hacimce %20 biyoetanol, %20 biyodizel, %60 dizel yakıtı), E30B20D50, E50B20D30 ve dizel yakıtı (D) kullanılmıştır. Testler tam gaz ve değişik motor devirlerinde yapılmıştır. Yapılan testler sonucu biyoetanol-biyodizel-dizel yakıtı karışımlarının kullanımında motor gücü, motor torku, karbon monoksit (CO), hidrokarbon (HC) ve duman yoğunluğu değerlerinde azalmalar olduğu tespit edilmiştir. Azot oksit (NO<sub>x</sub>) ve özgül yakıt tüketim değerleri ise artmıştır. Yanma karakteristikleri incelendiğinde değerlerin birbirine yakın olduğu görülmüştür.

**Anahtar Kelimeler:** Biyoetanol, aspir biyodizel, common rail dizel motor, yanma karakteristikleri

### NOMENCLATURE

ASTM	American Standards for Testing Materials
ATDC	after top dead center
BSFC	brake specific fuel consumption (g/kWh)
CO	carbon monoxide
CO <sub>2</sub>	carbon dioxide
D	100% diesel fuel
HC	hydro carbon
NO <sub>x</sub>	nitrogen oxides
LHV	lower heating value (MJ/kg)
Pe	Engine power (kW)
PM	particulate matter
ppm	particulate per million
rpm	revolution per minute
hrr	heat release rate
TTq	torque
E20B20D60	20% bioethanol, 20% biodiesel, 60% diesel by volume

E30B20D50	30% bioethanol, 20% biodiesel, 50% diesel by volume
E50B20D30	50% bioethanol, 20% biodiesel, 30% diesel by volume

### INTRODUCTION

Today, diesel engines are widely used in transportation, industry and agricultural areas because of their high fuel efficiency and ease of operation (Demirbas, 2008). The demand for diesel engines has been continuing to increase worldwide as a result of expanding industrialization (Ma et al., 2013). This is because diesel engines have certain advantages compared to spark ignition engines such as low fuel consumption, high engine torque and longevity (Park and Lee, 2013). Despite these advantages, today diesel engines are among the leading factors that cause air pollution (Fahd et al.,

2013; Torregrosa et al., 2013). In our day, studies are conducted on changing certain engine operating parameters such as valve timing, injection timing and rate in order to decrease harmful emissions (Barabás et al., 2010). In addition, researchers have been conducting studies on various renewable fuels such as biodiesel and alcohols because of the decrease in the reserves of fossil energy sources and their negative effects on the environment (Canakci et al., 2006; Hulwan and Joshi 2011; Breda 2011; Hazar 2010; Kannan et al., 2011).

Bioethanol, which is a type of alcohol, is obtained through the fermentation of agricultural products containing sugar and starch such as sugar beet, sugar cane, corn, wheat and wood-like plants (Park et al., 2012; Guido et al., 2013). The use of bioethanol in diesel engines provides a decrease in the amount of particulate matter (PM) in exhaust emissions (Hulwan and Joshi, 2011; Rahimi et al., 2009; Yilmaz and Sanchez, 2012). The decrease in PM (smoke) is related to the amount of oxygen contained in fuel blends (Shi et al., 2005). Biodiesel is a product which comes out as a result of the reaction of oils obtained from oilseed plants like canola, sunflower, soybean and safflower or of animal fats with a short-chain alcohol (methanol or ethanol) accompanied by a catalyst and used as fuel (Brunschwig et al., 2012; Acaroglu and Aydogan 2012). The biggest advantage in the use of biodiesel fuel is that it can be used without performing any modifications on the engine (Qi et al., 2010; Aydogan et al., 2011). Bioethanol, however, has a low cetane number. For this reason, its direct use in unmodified diesel engines is inconvenient (Aydogan, 2011). A review of the studies in the literature show that a good number of researchers focused on the use of ethanol in diesel engines. Shi et al. (2006) investigated the effects of ethanol-biodiesel-diesel fuel blends on engine emissions. In their study, they stated that the amount of PM in exhaust emissions decreased, whereas an increase was observed in the amount of carbon dioxide (CO<sub>2</sub>). Bhale et al. (2009) investigated the effects of mahua biodiesel and ethanol blends on engine performance and emissions. It was stated that CO and NO<sub>x</sub> emissions

decreased, whereas HC emissions increased as the result of the experiments conducted by using diesel fuel containing 20% ethanol. Lu et al. (2005) and Yan et al. (2009) reported that the use of bioethanol in diesel engines caused an increase in ignition delay and decreased the amount of NO<sub>x</sub> emissions. Xu et al. (2007) found that brake thermal efficiency increased depending on the increase in the percentage of bioethanol in fuel blends. Mohammadi et al. (2005) stated that NO<sub>x</sub> and PM emissions decreased, whereas HC and CO emissions increased with the use of bioethanol and diesel fuel blends.

When previous studies are examined, it can be seen that most of the researchers used bioethanol at a low ratio in diesel-bioethanol blends. The aim of the present study is to increase the percentage of the bioethanol used in diesel engines by adding biodiesel to diesel-bioethanol blends. Fuel blends were tested in a diesel engine with a common rail fuel injection system and the changes in cylinder pressure values were examined. Bioethanol, diesel fuel and safflower biodiesel were used as fuel. Safflower biodiesel was obtained from safflower oil through transesterification.

## EXPERIMENTAL APPARATUS AND PROCEDURE

Low-sulfur diesel fuel (Euro diesel) was purchased for the tests. Bioethanol produced from sugar beet was obtained from Konya Seker Inc. Safflower oil was used for producing biodiesel. Safflower oil was processed into biodiesel through transesterification. Three different fuel blends were prepared by using these fuels. The ratios of the fuel blends used in the experiments were determined based on the suggestions provided in previous studies. Density, kinematic viscosity and lower heating value (LHV) of the prepared fuel blends were measured. Fuel blends and their properties are presented in Table 1. The fuel blends were prepared right before the experiments in order to ensure homogeneity. Furthermore, the fuel in the tank was mixed using a mixer in order to prevent phase separation.

**Table 1.** Some properties of the test fuels

Fuel property	D	E20B20D60	E30B20D50	E50B20D30	Measurement method
Bioethanol content (%)	0	20	30	50	
Biodiesel content (%)	0	20	20	20	
Diesel Fuel content (%)	100	60	50	30	
Density (kg/m <sup>3</sup> ) at 15 °C	826.7	839.2	835.1	825.1	ASTM D4052
Kinematic Viscosity (mm <sup>2</sup> /s) at 40 °C	2.8221	2.4645	2.4853	2.0139	ASTM D445
Lower heating value (MJ/kg)	45.521	39.322	38.966	34.131	ASTM D240

A water-cooled, turbocharged diesel engine with an intercooler and a common rail fuel injection system was used in the study. The schematic diagram of the experimental setup used in the study is presented in Fig. 1. All the experiments were conducted without performing any modifications on the engine. The technical specifications of the test engine are presented in Table 2. An AVL GH13P/AG04 cylinder pressure sensor and AVL 365C Crank angle encoder were installed on

the test engine. Afterwards, the test engine was connected to a hydraulic dynamometer. Fuel consumption was measured by using a Dikomsan™ JS-B model electronic scale. A digital chronometer was used in order to determine the fuel consumption per unit time. An Orifice™ plate and differential pressure manometer was used to measure the air consumption of the engine.

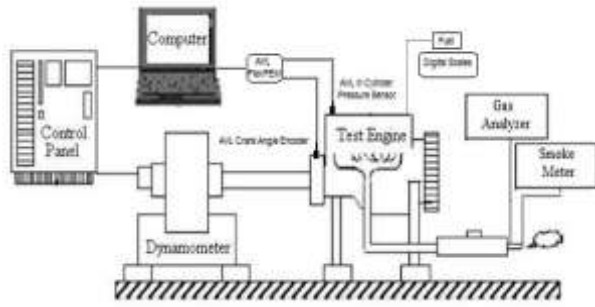


**Fig. 1.** The schematic diagram of the experimental setup

Exhaust temperatures were measured using a K-type thermocouple. Bosch BEA 350 gas analyzer and Bosch RTM 430 smoke meter were used to measure the exhaust emissions. The specifications of the measuring devices and the calculated uncertainty values are presented in Table 3. All the tests were conducted at full-throttle opening. Before starting the tests, the engine was operated until it reached a stable condition. Afterwards, the experiments were started. Engine speed, engine power, engine torque, fuel consumption and exhaust emission values were recorded during the experiment. During the measurement of the in-cylinder gas pressure, the pressure values were recorded at each 0.5 degree of the crankshaft through 120 cycles and the mean values

were calculated. The relative humidity, ambient temperature and pressure of the test room were measured using a hygrometer, a thermometer and a barometer, respectively. Fuel pump, fuel pipes and the fuel filter were emptied at each fuel change. All the experiments were repeated for three times and the means of the obtained values were calculated. Uncertainty analysis is applied to the experimental results (Holman, 2011). The details of the estimated uncertainty of calculated parameters are given in table 4.

**Table 2.** Specifications of the test engine

Engine type	Water-cooled, four stroke, turbo charged, intercooler, common rail fuel system
Number of cylinders	4
Cylinder volume	1910 cm <sup>3</sup>
Bore and stroke	82 x 90.4 (mm)
Compression ratio	18.5/1
Maximum torque	200 Nm@1750 rpm
Maximum power	77 kW@4000 rpm
Number of holes in nozzle	4
Size of nozzle	0.132 mm

**Table 3.** Technical details of the measuring equipment

Equipment	Method	Measurement	Upper limit	Accuracy	Uncertainty
Bosch BEA 350	Non-dispersive infrared	CO	10.00 vol.%	0.001 vol.%	0.002 vol.%
	Non-dispersive infrared	CO <sub>2</sub>	18.00 vol.%	0.001 vol.%	0.150 vol.%
	Non-dispersive infrared	HC	9999 ppm vol.	1 ppm vol.	2 ppm vol.
	Electro-chemical transmitter	NO	5000 ppm vol.	1 ppm vol.	21 ppm vol.
Bosch RTM 430	Photodiode receiver	Smoke opacity	100%	0.1%	0.8%
Load Cell	Strain gauge type load cell	Load	600 Nm	0.1 Nm	0.25%
Speed meter	Magnetic pick up type	Speed	10,000 rpm	10 rpm	0.10%
scale	Electronic	Mass	30 kg	1 gr	0.10%
<b>Calculated</b>					
Engine Power			100 kW	0.1 kW	0.47%
BSFC				5 g/kWh	0.10%

**Table 4.** Average uncertainties of calculated parameters

Parameters	Uncertainty(%)
Power	5.1
Brake specific fuel consumption	5.5
Speed	1.5
Length and diameter	0.1
Chronometer	± 0.5

## RESULTS AND DISCUSSION

Engine power and BSFC can be calculated using the following equation (Zhu et al., 2010).

$$P_e = \frac{T_{iq} \times n}{9550} \quad (1)$$

$$b_e = \frac{\dot{m}_f}{P_e} \times 10^3 \quad (2)$$

Where  $P_e$  is the engine power in kW;  $T_{iq}$  is the engine torque in Nm;  $n$  is the engine rpm,  $b_e$  is the BSFC in g/kWh;  $\dot{m}_f$  is the mass consumption rate of fuel in kg/s. The variation of engine power depending on engine speed is presented in Fig. 2. As it can be seen in Fig. 2, the power curves are similar in shape. As a result of the tests, it was seen that the highest engine power was obtained at 3000 rpm with all types of fuels. At this engine speed, engine power was measured as 46.3 kW with the use of D fuel, 44 kW with the use of E20B20D60 and E30B20D50 fuels and 39.75 kW with the use of E50B20D30 fuel. Engine power showed a decrease as the percentage of the bioethanol in the fuel blends increased. The engine power obtained through the use of fuel blends was found to be approximately 15% lower compared to diesel fuel. The major reason for the decrease in engine power is the difference between the heating values of the fuels. As it can be seen in Table 1, LHV values of the fuels decreased as the ratio of bioethanol in the blend increased.

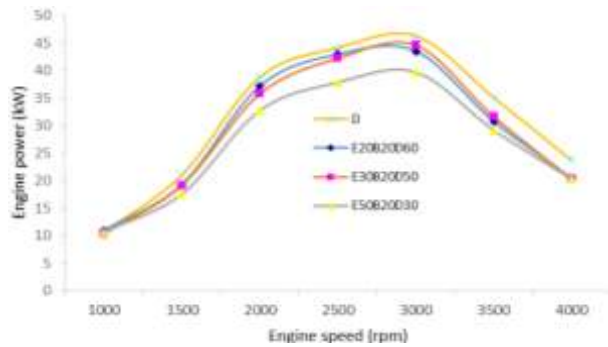


Fig. 2. Variation of engine power depending on engine speed

When we examine the engine torque values given in Fig. 3, we can see that a similar trend curve was formed with all types of fuels. The highest torque values were observed at 2000 rpm. Engine torque values showed a decrease as the ratio of the bioethanol in the fuel blend increased. At 2000 rpm, engine torque was measured as 185.59 Nm with D fuel, 175 Nm with E20B20D60 fuel, 170 Nm with E30B20D50 fuel and 153 Nm with E50B20D30 fuel. When we look at the lowest value, it is seen that there was an approximately 18% decrease compared to D fuel.

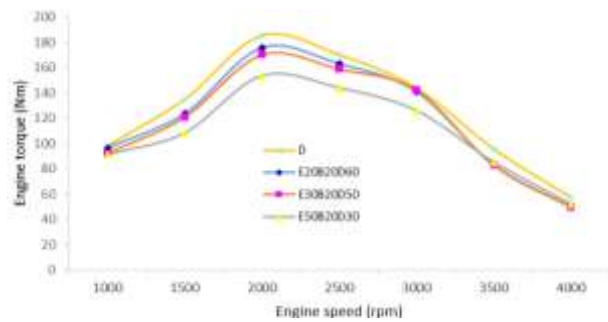


Fig. 3. Variation of engine torque depending on engine speed

The BSFC values presented in Fig. 4 show that the lowest value was obtained within the range of 2000-3000 rpm. Engine torque and engine power also reached the highest values at this speed range. As shown in Fig. 4, BSFC values increased as the ratio of bioethanol in the fuel blend increased. At 2500 rpm, the lowest BSFC value was 225 g/kWh with the use of D fuel, while the highest BSFC value was 267 g/kWh with the use of E50B20D30 fuel. This value is 18% higher compared to the BSFC value obtained with the use of D fuel. The amount of fuel used by the engine shows an increase as the heating value of the fuel increases (Stone, 1999; Zhu et al., 2010)

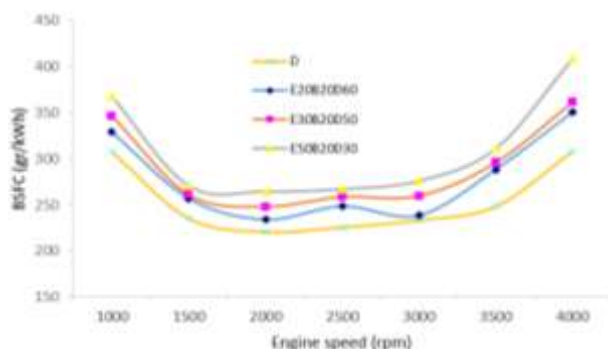


Fig. 4. Variation of BSFC values depending on engine speed

The CO emissions in exhaust gases represent the lost chemical energy that is not fully used in the engine (Soloiu, 2013). The variation of the CO values obtained in the experiments depending on engine speed is presented in Fig. 5. It can be seen that the curves representing the formation of CO emissions depending on engine speed are similar to one another for all fuel types. The highest CO value was measured at 1000 rpm. This can be explained by the fact that the cooling effect of the fuel causes a decrease in the temperature of the cylinder gasses especially at low engine speeds. As the engine speed increased, CO values started to decrease and reached the minimum value at 3000 rpm. There was no significant change at higher speeds. This decrease can be explained by the improvement of the air fuel ratio and the increase of engine load. As it is shown in Fig. 5, the highest CO values were obtained with D fuel, whereas these values started to decrease with the use of fuel blends depending on the increase in the ratio of bioethanol in the blend. The lowest CO values were measured with the use of E50B20D30 fuel. The chemical formula of bioethanol is  $C_2H_5OH$  (Aydogan, 2011). Therefore, it contains a certain amount of oxygen. Besides, biodiesel fuel also contains a certain amount of oxygen. Decreases of up to 80% were observed in the CO values of the bioethanol blends depending on the increase of the percentage of the oxygen in the fuel-air blend.

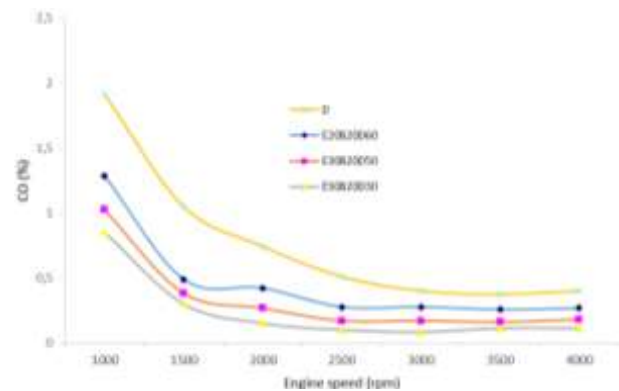


Fig. 5. Variation of CO values depending on engine speed

HC emissions in the exhaust gas occur due to the inefficient combustion of the fuel (Hsieh et al., 2002; Liberman, 2008; Armas et al., 2011). The variation of HC emission values depending on engine speed are presented in Fig. 6. HC emissions were found to be lower in all the blended fuels. According to the experimental results, the lowest HC emissions were measured at 3000 rpm as 27 ppm with D fuel, 15 ppm with E20B20D60 fuel, 12 ppm with E30B20D50 fuel and 9.8 ppm with E50B20D30 fuel. The reason for the low HC emissions of blended fuels can be explained by the oxygen content of bioethanol and biodiesel fuels. This oxygen causes an improvement in the combustion of the fuel. For this reason, the amount of HC in the exhaust gases decrease. Furthermore, it is thought that combustion speed varied depending on fuel type because the differences in fuel density and viscosity affect the fuel droplet size.

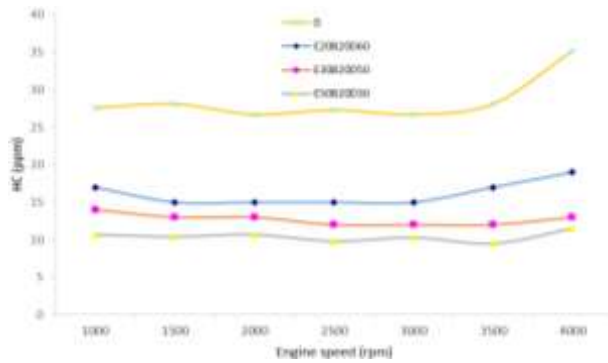


Fig. 6. Variation of HC values depending on engine speed

The most important problem in diesel engines is the  $\text{NO}_x$  emissions (Agarwal and Dhar, 2013). The high temperatures reached during the combustion in the cylinder combines the oxygen with the nitrogen in the air to form  $\text{NO}_x$  (Ajav at al., 1998; Challen and Baranescu, 1999; Andrea at al., 2004). Humidity has a large influence on  $\text{NO}_x$  emissions. Therefore, in this study, humidity in the air was continuously measured. The humidity correction factor for  $\text{NO}_x$  was calculated as stated by the Society of Automotive Engineers (Sae, 2001). The variation of  $\text{NO}_x$  emissions at different engine speeds is presented in Fig. 7.  $\text{NO}_x$  concentration first showed an increase depending on engine speed. However, it started to decrease after reaching the maximum torque speed. Maximum  $\text{NO}_x$  values were measured as 1488 ppm with the use of E50B20D30 fuel at 2500 rpm. This value was approximately 32% higher compared to the value obtained with D fuel. Bioethanol contains 34% oxygen 14. Furthermore, its low cetane number compared to that of diesel fuel increases the peak temperature in the cylinder (Qi at al., 2011). For this reason, the concentration of  $\text{NO}_x$  emissions increased with the use of all types of test fuels containing bioethanol.

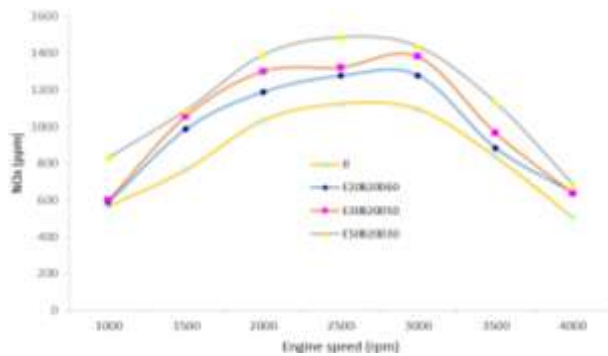


Fig. 7. Variation of  $\text{NO}_x$  values depending on engine speed

Smoke density emissions occur by the thermal cracking of the long-chain HC molecules in an oxygen-deficient combustion environment in the cylinder (Siwale at al., 2013). The oxygen content in the molecular structure of biological fuels is an important factor that affects smoke density (Ng at al., 2012). The smoke density values measured in the experiments are presented in Fig. 8. Decreases up to 85% were observed in smoke density values with the use of blended fuels. The main reason for the decrease in smoke density is that the oxygen content of the fuels maintains the required oxidation in the combustion environments.

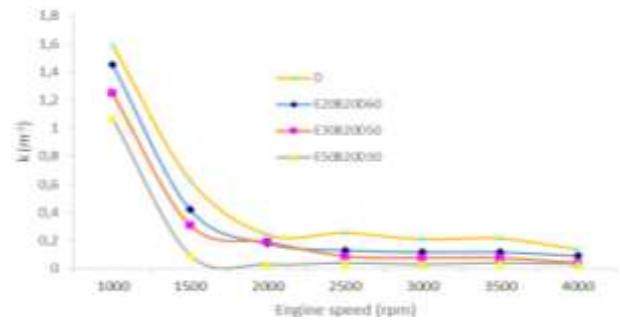


Fig. 8. Variation of smoke density values depending on engine speed

The combustion characteristics examined in the study were in-cylinder gas pressure, heat release rate and cumulative heat release rate. The distribution of the mechanical loads that occur in the cylinder as a result of the combustion of any type of fuel in an internal combustion engine depending on crank angle is represented by cylinder gas pressure curves (Zamboni and Capobianco, 2013). The in-cylinder gas pressure of the test engine was respectively measured at engine speeds of 1000, 2000, 3000 and 4000 rpm. The variation of cylinder gas pressure values depending on crank angle at different engine speeds is presented in Fig. 9-12. During the measurement of the in-cylinder pressure, the pressure values were recorded at each 0.5 degree of the crankshaft through 120 cycles and the mean values were calculated. Fig. 9 shows that the in-cylinder pressures at 1000 rpm and 2000 rpm were considerably similar to one another in all test fuels. When the pressure values at 3000 rpm and 4000 rpm are examined, it is seen that although the curves obtained with all types of test fuels were similar, maximum pressure values were found to be different. At 3000 rpm, peak cylinder pressure values occurred at approximately the same crank angle at 10 degrees after top dead center (ATDC). The highest pressure value was measured with the use of E30B20D50 fuel. The pressure values obtained with other fuels were relatively close to one another. Although the pressure values obtained at 4000 rpm were similar to one another, the peak cylinder pressure value was measured as 8.2 MPa for diesel fuel, whereas it was found to be between 9-9.3 MPa for blended fuels. The highest pressure value was obtained with the use of E50B20D30 fuel. This increase in the pressure values can be explained by the ratio of oxygen in the chemical structure of the E50B20D30 fuel blend.

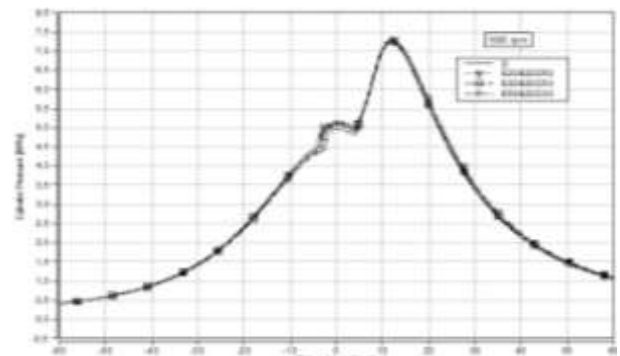
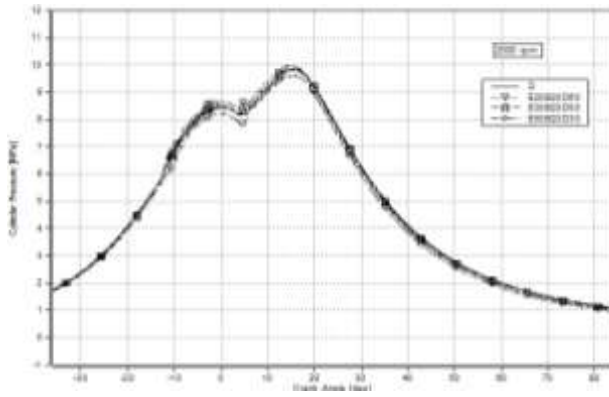
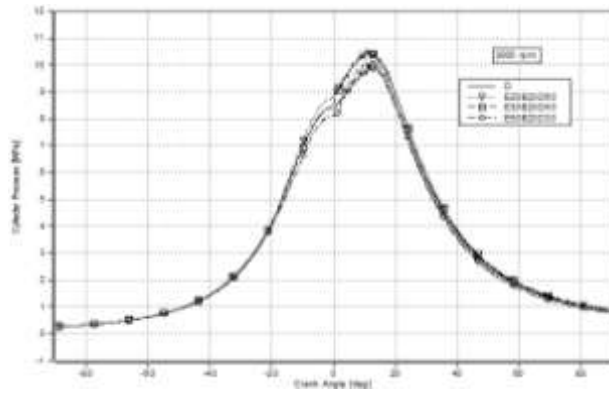


Fig. 9. Variation of cylinder gas pressure values depending on crank angle (1000 rpm)



**Fig. 10.** Variation of cylinder gas pressure values depending on crank angle (2000 rpm)



**Fig. 11.** Variation of cylinder gas pressure values depending on crank angle (3000 rpm)

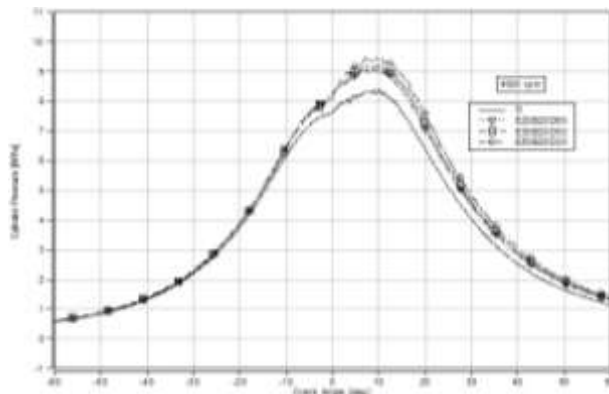


**Fig. 12.** Variation of cylinder gas pressure values depending on crank angle (4000 rpm)

Heat release calculations can be used to obtain information about the combustion process in an engine. There are several approaches in the literature regarding heat release analysis. One of the most commonly used approaches is the following equation developed by Krieger and Borman (Krieger and Borman 1966; Pulkrabek, 1997; Challen and Baranescu, 1999):

$$\dot{Q}_n = \frac{\lambda}{\lambda-1} P \frac{dV}{d\theta} + \frac{1}{\lambda-1} V \frac{dP}{d\theta} \quad (3)$$

In the equation,  $\lambda$  represents the ratio of specific heats and is calculated according to the empirical equation (Brunt et al., 1998).  $\theta$  is the crank angle,  $P$  is the cylinder gas pressure and  $V$  is the cylinder volume. In this model, heat release rate was calculated by applying the first law of thermodynamics to the control volume.

Cylinder volume was calculated as a function of the crank position. The calculated heat release rates are shown in Fig. 13-16.

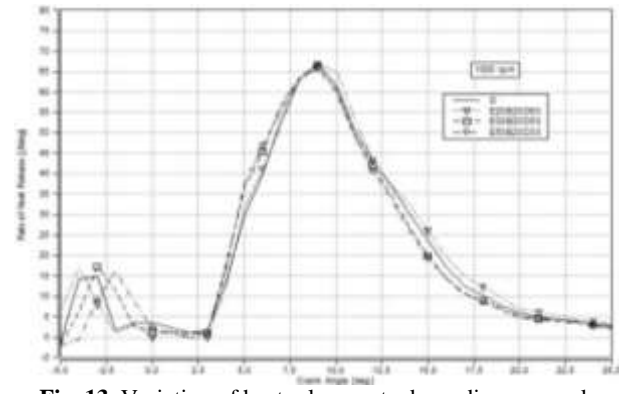


**Fig. 13.** Variation of heat release rate depending on crank angle (1000 rpm)

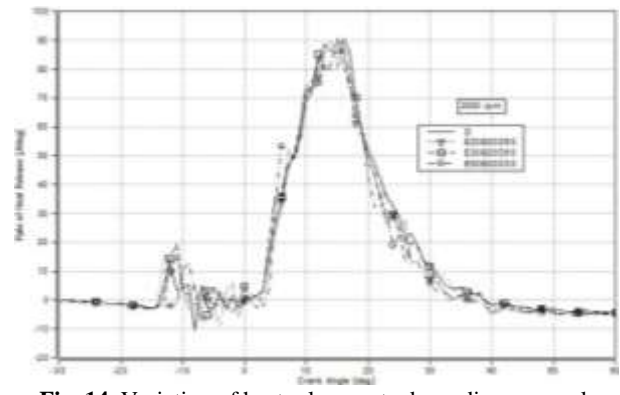


**Fig. 14.** Variation of heat release rate depending on crank angle (2000 rpm)

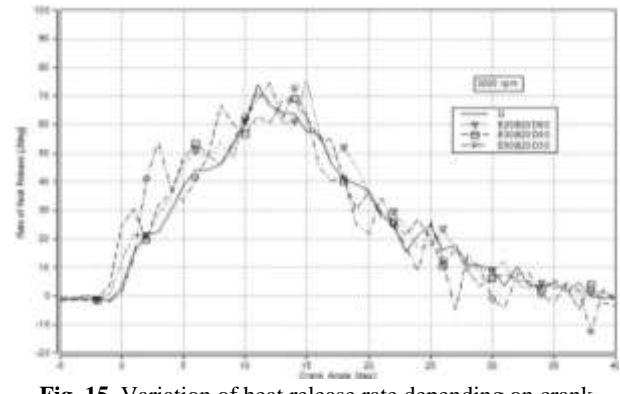


**Fig. 15.** Variation of heat release rate depending on crank angle (3000 rpm)

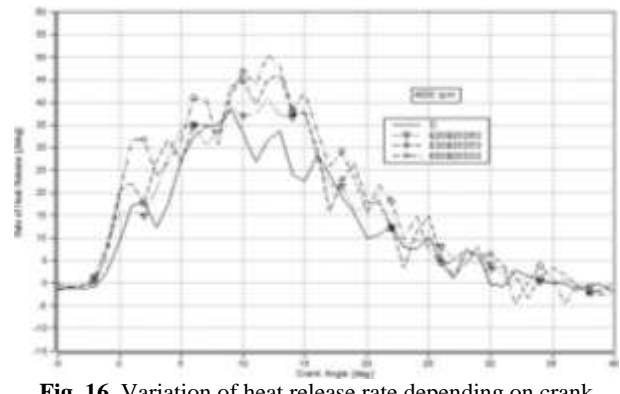


**Fig. 16.** Variation of heat release rate depending on crank angle (4000 rpm)

The heat release rate curves obtained at 1000 rpm and 2000 rpm show that peak heat release rate values were considerably close to one another. However, when we examine the section where the first injection was performed, we can see that the ignition delay time prominently increased especially with the use of E50B20D30 fuel. The values obtained at 3000 rpm show that although the peak heat release rate values were considerably close to one another, the times to reach the peak heat release rate were different. The fuel that first reached the peak heat release rate was diesel fuel. E50B20D30, E30B20D30 and E20B20D30 fuels followed diesel fuel in reaching the peak heat release rate, respectively. At 4000 rpm, the fuels with the highest peak heat release rate were E50B20D30, E30B20D30 and E20B20D30, respectively. Peak heat release rate was reached at 12 degrees ATDC with the use of E50B20D30 fuel, whereas this value was reached at 9 degrees ATDC with Diesel fuel. The values obtained at especially 3000 rpm and 4000 rpm show that Diesel fuel reached the peak heat release rate before other fuel blends. The cetane number of diesel fuel is higher than that of bioethanol. For this reason, diesel fuel might have reached the peak heat release rate earlier because of the fast combustion at the mentioned engine speeds.

Cumulative heat release rates are presented in Fig. 17-20. Negative values were obtained especially at 1000 rpm. Because of the vaporization of the fuel accumulated during ignition delay, a negative cumulative heat release is observed at the beginning of the curve but the heat release values become positive after combustion is initiated. Cumulative heat release rates showed an increase especially at 4000 rpm depending on the ratio of the bioethanol in the blend. This indicates inefficient conversion of thermal energy into shaft power for Bioethanol blends compared to diesel fuel.

## CONCLUSIONS

In the present study, engine performance, emission and combustion characteristics were investigated at different engine speeds in a 4-cylinder, water-cooled, four stroke, turbo charged diesel engine with an intercooler and a common rail fuel injection system. Bioethanol, safflower biodiesel and diesel fuel blends were used as test fuel. The results were compared with those obtained with diesel fuel. The main results can be summarized as follows:

1. Although decreases of up to 18% were observed in engine torque and engine power, increases of up to 18% were observed in BSFC values with the use of fuel blends.
2. Regarding exhaust emissions, decreases were observed in CO, HC and smoke density values.
3. Increases of up to approximately 32% were determined in NO<sub>x</sub> values compared to diesel fuel.
4. Combustion characteristics were found to be close to one another.
5. It was observed that bioethanol could be used in a diesel engine with a common rail fuel injection system at ratios of up to 50% by adding 20% biodiesel by volume without performing any modifications on the engine.

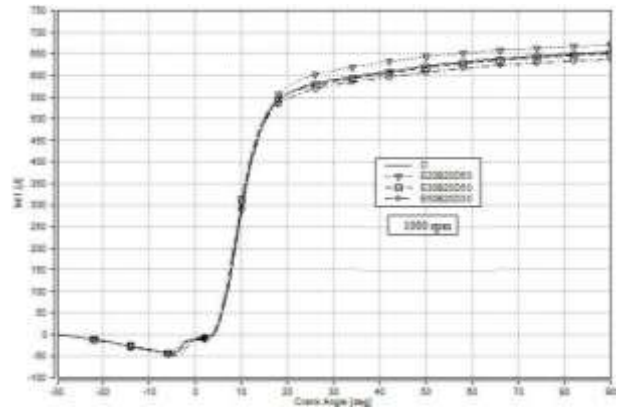


Fig. 17. Variation of cumulative heat release rate values depending on crank angle (1000 rpm)

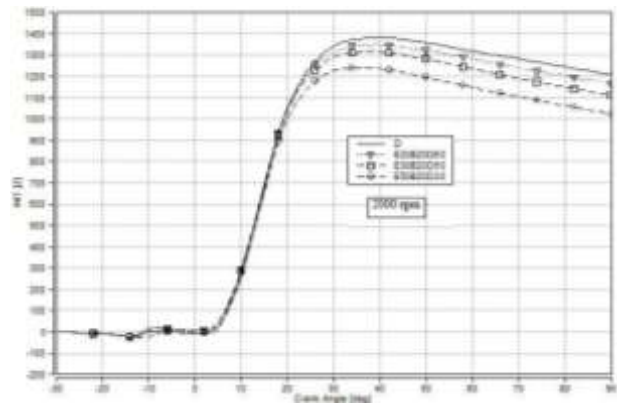


Fig. 18. Variation of cumulative heat release rate values depending on crank angle (2000 rpm)

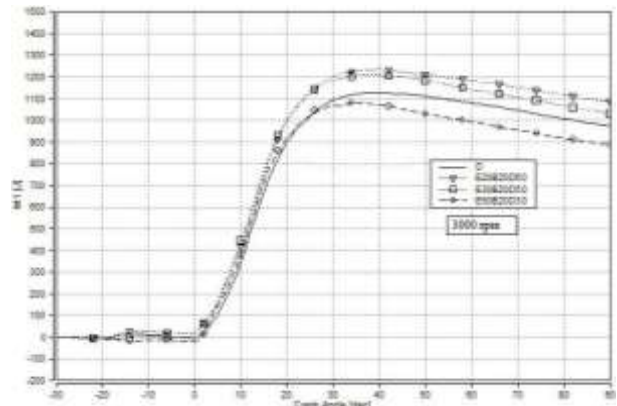


Fig. 19. Variation of cumulative heat release rate values depending on crank angle (3000 rpm)

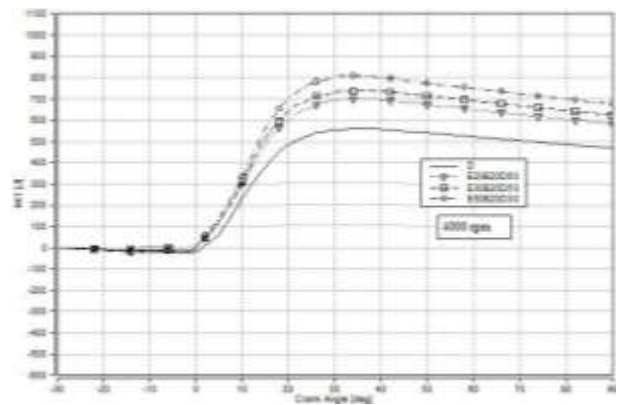


Fig. 20. Variation of cumulative heat release rate values depending on crank angle (4000 rpm)

## ACKNOWLEDGEMENTS

This study was supported by selcuk university scientific research projects center. (Project number:11401145)

## REFERENCES

- Acaroglu, M. and Aydogan, H. (2012). Biofuels energy sources and future of biofuels energy in Turkey, *Biomass & Bioenergy*, 36, 69-76.
- Agarwal, A. K. and Dhar, A. (2013). Experimental investigations of performance, emission and combustion characteristics of Karanja oil blends fuelled DI engine, *Renewable Energy*, 52, 283-291.
- Ajav, E. A., Singh, B. and Bhattacharya, T. K. (1998). Performance of a stationary diesel engine using vaporized ethanol as supplementary fuel, *Biomass & Bioenergy*, 15, 493-502.
- Andrea, T. D., Henshaw, P. F. and Ting, D. S. (2004). The addition of hydrogen to gasoline-fuelled SI engine, *International Journal of Hydrogen Energy*, 29, 1541-1552.
- Armas, O., Martínez-Martínez, S. and Mata, C. (2011). Effect of an ethanol-biodiesel-diesel blend on a common rail injection system, *Fuel Processing Technology*, 92, 2145-2153.
- Aydogan, H. (2011). Investigation of engine performance and exhaust emission effect using bioethanol-diesel fuel blends (E-Diesel), Ph.D. thesis, Selcuk University, Konya, Turkey, 1-25.
- Aydogan, H., Ozcelik, A. E. and Acaroglu, M. (2011). The effect of peanut oil methyl ester on the performance and emissions of a diesel engine with a pump injection fuel system, *Energy. Educ. Sci. Technol-Pt. A.*, 28, 189-200.
- Barabás, I., Todoruț, A. and Băldean, D. (2010). Performance and emission characteristics of an CI engine fueled with diesel-biodiesel-bioethanol blends, *Fuel*, 89, 3827-3832.
- Bhale, P. V., Deshpande, N. V., Thombre, S. B. (2009). Improving the low temperature properties of biodiesel fuel, *Renewable Energy*, 34, 794-800.
- Breda, K. (2011). Influence of biodiesel on engine combustion and emission characteristics, *Applied Energy*, 88, 1803-1812.
- Brunschwig, C., Moussavou, W. and Blin, J. (2012). Use of bioethanol for biodiesel production, *Progress in Energy and Combustion*, 38, 283-301.
- Brunt, M. F. J., Rai, H. and Emtage, A. L. (1998). The calculation of heat release energy from cylinder pressure data, *SAE Paper*, No. 981052.
- Canakci, M., Erdil, A. and Arcaklioglu, E. (2006). Performance and exhaust emissions of a biodiesel engine, *Applied Energy*, 83, 594-605.
- Canakci, M., Ozsezen, A. N. and Turkcan, A. (2009). Combustion analysis of preheated crude sunflower oil in an IDI diesel engine, *Biomass & Bioenergy*, Vol. 33, 760-767.
- Challen, B. and Baranescu, R. (1999). Diesel engine reference book, 2nd ed., England, Butterworth and Heinemann Publishing.
- Demirbas, A. (2008). Biofuels sources, biofuel policy, biofuel economy and global biofuel projections, *Energy Conversion and Management*, 49, 2106-2116.
- Fahd, M. E. A., Wenming, Y., Lee, P.S., Chou, S.K. and Yap, C. R. (2013). Experimental investigation of the performance and emission characteristics of direct injection diesel engine by water emulsion diesel under varying engine load condition, *Applied Energy*, 102, 1042-1049.
- Guido, C., Beatrice, C., Napolitano, P. (2013). Application of bioethanol/RME/diesel blend in a Euro5 automotive diesel engine, Potentiality of closed loop combustion control technology, *Applied Energy*, 102, 13-23.
- Hazar, H. (2010). Cotton methyl ester usage in a diesel engine equipped with insulated combustion chamber, *Applied Energy*, 87, 134-40.
- Holman, J. P., (2011), Experimental methods for engineers, 8th ed., McGraw-Hill series in mechanical engineering.
- Hsieh, W. D., Chen, R. H., Wu, T. L. and Lin, T. H. (2002). Engine performance and pollutant emission of an SI engine using ethanol-gasoline blended fuels, *Atmospheric Environment*, 36, 403-410.
- Hulwan, D. B. and Joshi, S. V. (2011). Performance, emission and combustion characteristic of a multicylinder DI diesel engine running on diesel-ethanol-biodiesel blends of high ethanol content, *Applied Energy*, 88, 5042-5055.
- Kannan, G.R., Karvembu, R. and Anand, R. (2011). Effect of metal based additive on performance emission and combustion characteristics of diesel engine fuelled with biodiesel, *Applied Energy*, 88, 3694-3703.
- Krieger, R. B. and Borman, G. L. (1966). The computation of applied heat release for internal combustion engines, *ASME Paper*, 66-WA/DGP-4.
- Lieberman, M. (2008). Introduction to physics and chemistry of combustion, Springer-Verlag, Berlin Heidelberg, pp 1-74.
- Lu, X., Huang, Z., Zhang, W. and Li, D. (2005). Combustion visualization and emissions of a direct injection compression ignition engine fueled with bio-diesohol, *Int. J. Auto. Tech-Kor.*, 6, 15-21.

- Ma, Y., Zhu, M. and Zhang D. (2013). The effect of a homogeneous combustion catalyst on exhaust emissions from a single cylinder diesel engine, *Applied Energy*, 102, 556-562.
- Mohammadi, A., Kee, S., Ishiyama, T., Kakuta, T. and Matsumoto, T. (2005). Implementation of ethanol diesel blend fuels in PCCI combustion, *SAE tech paper*, 2005-01-3712.
- Ng, J. H., Ng, H. K. Gan, and S. (2012). Characterisation of engine-out responses from a light-duty diesel engine fuelled with palm methyl ester (PME), *Applied Energy*, 90, 58-67.
- Park, S. H., Cha, J. and Lee, C. S. (2012). Impact of biodiesel in bioethanol blended diesel on the engine performance and emissions characteristics in compression ignition engine, *Applied Energy*, 99, 334-343.
- Park, S. H. and Lee, C. S. (2013). Combustion performance and emission reduction characteristics of automotive DME engine system, *Progress in Energy and Combustion*, 39, 147-168.
- Pulkrabek, W. W. (1997). Engineering fundamentals of the internal combustion engine, 2nd ed., New Jersey, Prentice-Hall.
- Rahimi, H., Ghobadian, B., Yusaf, T., Najafi, G. and Khatamifar, M. (2009). Diesterol, an environment friendly IC engine fuel, *Renewable Energy*, 34, 335-342.
- SAE. SAE handbook, (2001). MI 1, Warrendale, SAE, 1304-1306.
- Shi, X., Yu, Y., He, H., Shuai, S., Wang, J. and Li, R. (2005). Emission characteristics using methyl soyate-ethanol-diesel fuel blends on a diesel engine, *Fuel*, 84, 1543-1549.
- Shi, X., Pang, X., Mu, Y., He, H., Shuai, S., Wang, J., Chen, H. and Li, R. (2006). Emission reduction potential of using ethanol-biodiesel-diesel fuel blend on a heavy-duty diesel engine, *Atmospheric Environment*, 40, 2567-2574.
- Siwale, L., Kristóf, L., Adam, T., Bereczky, A., Mbarawa, M., Penninger, A. and Kolesnikov, A. (2013). Combustion and emission characteristics of n-butanol/diesel fuel blend in a turbo-charged compression ignition engine, *Fuel*, 107, 409-418.
- Soloiu, V., Duggan, M., Harp, S., Vlcek, B. and Williams, D. (2013). PFI (port fuel injection) of n-butanol and direct injection of biodiesel to attain LTC (low-temperature combustion) for low-emissions idling in a compression engine, *Energy*, 52, 143-154.
- Stone, R. (1999). Introduction to internal combustion engines, 3rd ed., New York, Macmillan.
- Torregrosa, A.J., Broatch, A., Plá, B. and Mónico, L.F. (2013). Impact of Fischer-Tropsch and biodiesel fuels on trade-offs between pollutant emissions and combustion noise in diesel engines, *Biomass & Bioenergy*, 52, 22-33.
- Qi, D. H., Chen, H., Matthews, R. D. and Bian, Y. Z. H. (2010). Combustion and emission characteristics of ethanol-biodiesel-water micro-emulsions used in a direct injection compression ignition engine, *Fuel*, 89, 958-964.
- Qi, D. H., Chen, H., Geng, L. M. and Bian, Y. Z. (2011). Effect of diethyl ether and ethanol additives on the combustion and emission characteristics of biodiesel-diesel blended fuel engine, *Renewable Energy*, 36, 1252-1258.
- Xu, B. Y., Qi, Y. L., Zhang, W.B. and Cai, S.L. (2007). Fuel properties and emissions characteristics of ethanol-diesel blend on small diesel engine, *Int. J. Auto. Tech-Kor.*, 8, 9-18.
- Yan, Y., Zhang, Y., Rao, S., Zhang, R. and Wu, D. (2009). Study of combustion and emission characteristics of diesel engines fueled with ethanol/diesel blended fuel, *SAE tech paper*, 2009-01-2675.
- Yilmaz, N. and Sanchez, T. M. (2012). Analysis of operating a diesel engine on biodiesel-ethanol and biodiesel-methanol blends, *Energy*, 46, 126-129.
- Zamboni, G. and Capobianco, M. (2013). Influence of high and low pressure EGR and VGT control on in-cylinder pressure diagrams and rate of heat release in an automotive turbocharged diesel engine, *Applied Thermal Engineering*, 51, 586-596.
- Zhu, L., Cheung, C.S., Zhang, W.G. and Huang, Z. (2010). Emissions characteristics of a diesel engine operating on biodiesel and biodiesel blended with ethanol and methanol, *Science of the Total Environment*, 408, 914-921.



Hasan AYDOGAN was born in Eskişehir. He is Assistant Professor Doctor at the Selcuk University, Technology Faculty in Konya. His main scientific interests include biofuels diesel engine, renewable energy.